

# Push–Pull $\pi$ -Electron Phosphonic-Acid-Based Self-Assembled Multilayer Nanodielectrics Fabricated in Ambient for Organic Transistors

Young-geun Ha, Antonio Facchetti,\* and Tobin J. Marks\*

Department of Chemistry and Materials Research Center,  
Northwestern University, 2145 Sheridan Road,  
Evanston, Illinois 60208

Received November 15, 2008

Revised Manuscript Received January 21, 2009

Organic thin-film transistors (OTFTs) are of great current interest for future organic electronics applications such as RF-ID cards, flexible displays, and sensors.<sup>1</sup> Despite recent progress, large OTFT operating voltages, reflecting the intrinsically low mobilities of organic semiconductors, remain one of the major challenges to overcome.<sup>2</sup> For portable applications such as RF-ID tags and displays, it is mandatory to achieve high TFT drain currents ( $I_{SD}$ ) at acceptably low operating voltages. Several approaches have been proposed to achieve these goals,<sup>3</sup> one of which is to reduce channel lengths due to the inverse proportionality between  $I_{SD}$  and the channel length. However, this approach requires expensive lithographies to pattern small features and commensurate scaling of the gate dielectric thickness. For the same device geometry and semiconductor material, equivalent OTFT  $I_{SD}$  parameters should be achievable at lower operating voltages by increasing the gate dielectric capacitance  $C_i$ , given by eq 1, where  $\epsilon_0$  is the vacuum permittivity,  $k$  is the dielectric constant, and  $d$  is the thickness of dielectric layer.

$$C_i = \epsilon_0 k/d \quad (1)$$

Several approaches have been used to increase  $C_i$ , each of which has its own advantages and limitations. These include using high- $k$  metal oxides,<sup>4a–c</sup> polymer–inorganic composites,<sup>4d</sup> and ion-gel electrolytes.<sup>4e</sup> However, these approaches

typically require either high growth temperatures and/or relatively thick films to ensure sufficiently low gate leakage currents. Therefore, a promising method to lower the operating voltages is to use solution-processed ultrathin gate dielectric films fabricated near room temperature, thereby affording high capacitances with low leakage currents. Several groups have recently reported low operating voltage OTFTs using self-assembled monolayer (SAM)<sup>5</sup> and spin-coated polymer dielectrics.<sup>6</sup>

Contemporaneously, this research group reported self-assembled nanodielectrics (SANDs), fabricated from silane precursors and consisting of alternating organic–inorganic multilayers chemically bound by strong siloxane linkages.<sup>7</sup> These dielectrics are compatible with organic semiconductors, single-walled carbon nanotubes, and a variety of inorganic semiconductors.<sup>8</sup> The SAND multilayer structures containing “push–pull” polarizable  $\pi$ -electron building blocks enhance capacitance, depress leakage current and interface trap densities, and significantly enhance inorganic semiconductor TFT performance.<sup>8b,c</sup>

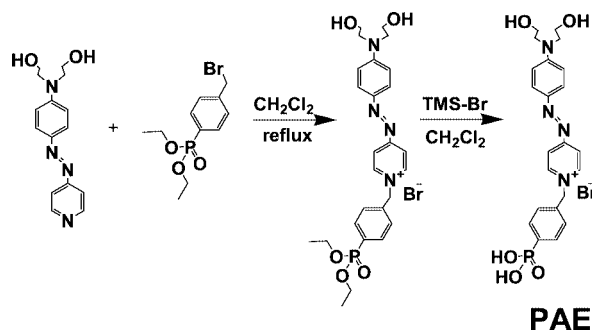
A significant limitation of the organo-chlorosilane-based SAND self-assembly approach is that it uses ambient-sensitive precursors that must be applied using dry solvents under an inert atmosphere. Therefore, the question arises as to whether it might be possible to use alternative, ambient-compatible reagents to fabricate high-performance multilayer nanodielectrics. In this contribution, we report the synthesis and implementation of inorganic–organic hybrid multilayer gate dielectrics for OTFTs, prepared using phosphonic-acid-functionalized organic precursors. These reagents are well-suited for ambient atmosphere self-assembly of nanoscopic multilayers and, compared to conventional alkyl SAM precursors, include highly polarizable,  $k$ -enhancing<sup>5a</sup> stilbazolium groups within the nanoscopic layers. We show that the resulting, structurally well-defined films (p-SANDS) are

\* Corresponding authors. E-mail: t-marks@northwestern.edu (T.J.M); a-facchetti@northwestern.edu (A.F.).

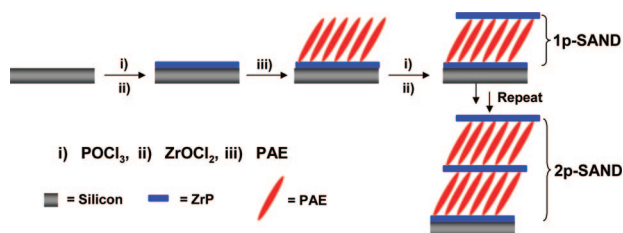
- (1) (a) Roberts, M. E.; Mannsfeld, S. C. B.; Queralto, N.; Reese, C.; Locklin, J.; Knoll, W.; Bao, Z. *Proc. Natl. Acad. Sci. U.S.A.* **2008**, *105*, 12134. (b) Murphy, A. R.; Frechet, J. M. J. *Chem. Rev.* **2007**, *107*, 1066. (c) Zaumseil, J.; Sirringhaus, H. *Chem. Rev.* **2007**, *107*, 1066. (d) Kim, C.; Facchetti, A.; Marks, T. J. *Science* **2007**, *318*, 76. (e) Lee, J.; Panzer, M. J.; He, Y.; Lodge, T. P.; Frisbie, C. D. *J. Am. Chem. Soc.* **2007**, *129*, 4532. (f) De Leeuw, D. M. *Nat. Mater.* **2004**, *3*, 106.
- (2) (a) Schmidt, R.; Ling, M. M.; Oh, J. H.; Winkler, M.; Könnemann, M.; Bao, Z.; Würthner, F. *Adv. Mater.* **2007**, *19*, 3692. (b) McCulloch, I.; Heeney, M.; Bailey, C.; Genevicius, K.; Macdonald, I.; Shkunov, M.; Sparrowe, D.; Tierney, S.; Wagner, R.; Zhang, W. M.; Chabiny, M. L.; Kline, R. J.; McGehee, M. D.; Toney, M. F. *Nat. Mater.* **2006**, *5*, 328. (c) Katz, H. E.; Lovinger, A. J. *Nature* **2000**, *404*, 478.
- (3) (a) Haas, U.; Gold, H.; Haase, A.; Jakopic, G.; Stadlober, B. *Appl. Phys. Lett.* **2007**, *95*, 043511. (b) Tulevski, G. S.; Nuckolls, C.; Afzali, A.; Graham, T. O.; Kagan, C. R. *Appl. Phys. Lett.* **2006**, *89*, 183101.

- (4) (a) Wang, G.; Moses, D.; Heeger, A. J.; Zhang, H.-M.; Narasimhan, M.; Demaray, R. E. *J. Appl. Phys.* **2004**, *95*, 316. (b) Lee, J.; Kim, J. H.; Im, S. *Appl. Phys. Lett.* **2003**, *83*, 2689. (c) Tate, J.; Rogers, J. A.; Jones, C. D. W.; Vyas, B.; Murphy, D. W.; Li, W.; Bao, Z.; Slusher, R. E.; Dodabalapur, A.; Katz, H. E. *Langmuir* **2000**, *16*, 6054. (d) Maliakal, A.; Katz, H.; Cotts, P. M.; Subramoney, S.; Mirau, P. *J. Am. Chem. Soc.* **2005**, *127*, 14655. (e) Panzer, M. J.; Frisbie, C. D. *Adv. Mater.* **2008**, *20*, 3177.
- (5) (a) DiBenedetto, S. A.; Frattarelli, D.; Ratner, M. A.; Facchetti, A.; Marks, T. J. *J. Am. Chem. Soc.* **2008**, *130*, 7528. (b) Park, Y.; Kim, D.; Jang, Y.; Hwang, M.; Cho, K. *Appl. Phys. Lett.* **2005**, *87*, 243509. (c) Halik, M.; Klauk, H.; Zschieschang, U.; Schmid, G.; Dehm, C.; Schütz, M.; Maisch, S.; Effenberger, F.; Brunnbauer, M.; Stellacci, F. *Nature* **2004**, *431*, 963. (d) Collet, J.; Tharaud, O.; Chapoton, A.; Vuillaume, D. *Appl. Phys. Lett.* **2000**, *76*, 1941.
- (6) (a) Jeon, Y.; Cho, K. *Appl. Phys. Lett.* **2006**, *88*, 072101. (b) Yoon, M. H.; Yan, H.; Facchetti, A.; Marks, T. J. *J. Am. Chem. Soc.* **2005**, *127*, 10388. (c) Klauk, H.; Halik, M. *J. Appl. Phys.* **2002**, *92*, 5259.
- (7) Yoon, M. H.; Facchetti, A.; Marks, T. J. *Proc. Natl. Acad. Sci.* **2005**, *102*, 4678.
- (8) (a) Ju, S.; Li, J.; Liu, J.; Chen, P. C.; Ha, Y.-G.; Ishikawa, F.; Chang, H.; Zhou, C.; Facchetti, A.; Janes, D. B.; Marks, T. J. *Nano Lett.* **2008**, *8*, 997. (b) Byrne, P.; Facchetti, A.; Marks, T. J. *Adv. Mater.* **2008**, *20*, 2319. (c) Kim, H.; Byrne, P.; Facchetti, A.; Marks, T. J. *J. Am. Chem. Soc.* **2008**, *130*, 12508. (d) Wang, L.; Yoon, M.-H.; Facchetti, A.; Marks, T. J. *Nat. Mater.* **2007**, *6*, 317. (e) Hur, S. H.; Yoon, M. H.; Gaur, A.; Shim, M.; Facchetti, A.; Marks, T. J.; Rogers, J. A. *J. Am. Chem. Soc.* **2005**, *127*, 13808.

### Scheme 1. Synthesis of Polarizable Phosphonic Acid-Based p-SAND $\pi$ -Electron Building Block



### Scheme 2. Self-Assembly Procedure for 1p-SAND and 2p-SAND Multilayer Nanodielectrics



excellent gate dielectrics for TFT applications, exhibiting high capacitances and low leakage current densities.

Phosphonic-acid-based SAMs for OTFT gate dielectrics were first reported by Klauk<sup>9a</sup> using single monolayers of *n*-octadecylphosphonic acid deposited on Al/Al<sub>2</sub>O<sub>3</sub> substrates, and implemented by the same group<sup>9a</sup> in low-power organic circuits and more recently by Jen et al.<sup>9b</sup> In this contribution, we take a different approach to **p-SAND** multilayer nanodielectrics. Phosphonic-acid-based organic–inorganic multilayers containing highly polarizable, phosphonic “push–pull”  $\pi$ -electron layers (**PAE**) intercalated between robust inorganic zirconium phosphonate (**ZrP**) interlayers (to impart chromophore layer orientational stability) are self-assembled under ambient. The **PAE**–**ZrP** interlayer bonding is based on the insoluble, layered salts formed by organic phosphonic acids with Zr<sup>4+</sup> and other metal ions.<sup>10</sup>

The new **PAE**  $\pi$ -electron precursor 4-[[4-[bis(2-hydroxyethyl)amino]phenyl]diazanyl]-1-(4-phosphono-benzyl) pyridinium bromide was synthesized by the procedure outlined in Scheme 1 and characterized by conventional analytical/spectroscopic techniques (see the Supporting Information for synthetic and characterization details).

In the present multilayer synthetic approach, a **ZrP** primer layer is first deposited by exposing the substrate surface hydroxyl groups to POCl<sub>3</sub> and then to a ZrOCl<sub>2</sub> solution. Self-assembled nanodielectric layers are then fabricated according to Scheme 2, first depositing the **ZrP** primer layer on a silicon wafer, and then the phosphonic-acid-based  $\pi$ -electron (**PAE**) layer, followed by the **ZrP** interlayer for capping and further self-assembly. This procedure is a modification of the multilayer synthetic approach originally

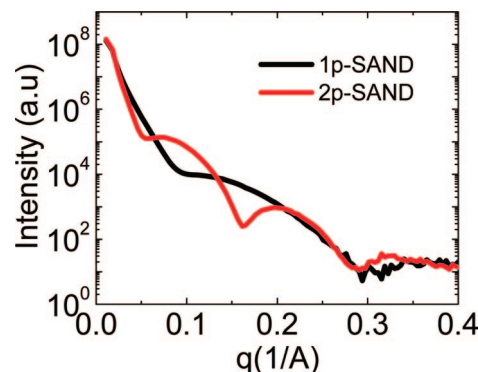


**Figure 1.** X-ray reflectivity data for **p-SAND** nanodielectric films on substrates. Film thicknesses are estimated from the fringe positions.

developed by Katz<sup>11</sup> and Mallouk.<sup>12</sup> Specifically, clean, heavily doped *n*-type silicon substrates are immersed in a CH<sub>3</sub>CN solution of 0.2 M POCl<sub>3</sub>–0.2 M collidine at 25 °C for 18 h, rinsed with DI H<sub>2</sub>O, zirconated in 5 mM aqueous ZrOCl<sub>2</sub> solution at room temperature for 2 h, and finally rinsed again with DI H<sub>2</sub>O to complete the **ZrP** primer layer. Next, the primer layer coated substrate is immersed in a 3 mM MeOH solution of the phosphonic acid  $\pi$ -electron stilbazolium reagent (**PAE**) at 60 °C for 2 h and rinsed with MeOH; the capping zirconium phosphonate layer is then applied as described above, affording **1p-SAND**. A bilayer phosphonic-acid-based SAND (**2p-SAND**) can be fabricated by repeating this sequence.

The X-ray reflectivity-derived thicknesses of the **p-SANDs** are  $\sim 3.0$  nm (**1p-SAND**) and  $\sim 5.6$  nm (**2p-SAND**) (Figure 1). Atomic force microscopic (AFM) images of the **1p-SAND** and **2p-SAND** surfaces are consistent with crack/pinhole-free morphologies. The maximum rms roughness is 0.6 nm (**1p-SAND**) and 0.9 nm (**2p-SAND**), respectively (see Figure S1 in the Supporting Information). To quantify **p-SAND** dielectric properties, we fabricated metal–insulator–semiconductor (MIS) sandwich structures by Au contact (200  $\mu\text{m} \times 200 \mu\text{m}$ ) vapor deposition on **p-SAND**-coated Si substrates. The MIS leakage current density (*J*) and capacitance are shown in Figure 2. Compared to **1p-SAND**, which exhibits current densities of  $1 \times 10^{-3}$  to  $1 \times 10^{-5}$  A/cm<sup>2</sup> at  $\pm 2$  V, **2p-SAND** affords lower leakage current densities by  $\sim 100\times$  for the same bias window ( $1 \times 10^{-5}$  to  $1 \times 10^{-6}$  A/cm<sup>2</sup>), probably reflecting some combination of tunneling and defect healing. Note however, that the roughness of the first **1p-SAND** layer renders the second layer less dense and probably less defect-free, and thus more susceptible to current leakage. Capacitance measurements performed on these MIS structures afford values of 700 nF/cm<sup>2</sup> for **1p-SAND** and 520 nF/cm<sup>2</sup> for **2p-SAND** in the accumulation regime (0 to +1.0 V), far greater than the

(9) (a) Klauk, H.; Zschieschang, U.; Pflaum, J.; Halik, M. *Nature* **2007**, *445*, 745. (b) Ma, H.; Acton, O.; Ting, G.; Ka, J. W.; Yip, H. L.; Tucker, N. M.; Schofield, R.; Jen, A.K.-Y. *Appl. Phys. Lett.* **2008**, *92*, 113303.

(10) Dines, M. B.; DiGiacomo, P. M. *Inorg. Chem.* **1981**, *20*, 92.

(11) (a) Katz, H. E.; Scheller, G.; Putvinski, T. M.; Schilling, M. L.; Wilson, W. L.; Chidsey, C. E. D. *Science* **1991**, *254*, 1485. (b) Schilling, M. L.; Katz, H. E.; Stein, S. M.; Shane, S. F.; Wilson, W. L.; Ungashe, S. B.; Taylor, G. N.; Putvinski, T. M.; Chidsey, C. E. D.; Buratto, S. *Langmuir* **2003**, *9*, 2156. (c) Katz, H. E.; Schilling, M. L. *Chem. Mater.* **1993**, *5*, 1162. (d) Katz, H. E.; Scheller, G.; Putvinski, T. M.; Schilling, M. L.; Wilson, W. L.; Chidsey, C. E. D. *Chem. Mater.* **1991**, *3*, 699.

(12) (a) Lee, H.; Kepley, L.; Hong, H.; Akhter, S.; Mallouk, T. E. *J. Phys. Chem.* **1988**, *92*, 2597. (b) Lee, H.; Kepley, L.; Hong, H.; Mallouk, T. E. *J. Am. Chem. Soc.* **1988**, *110*, 618.

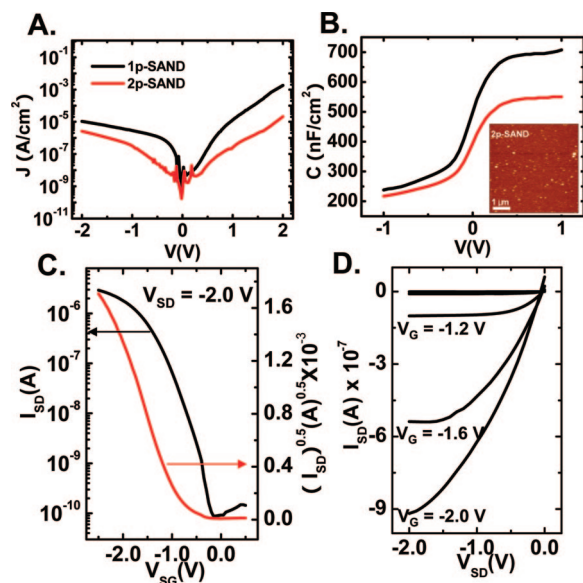


**Figure 2.** (A) Leakage current density vs voltage; (B) capacitance vs voltage at 10 kHz for **1p-SAND**- (red) and **2p-SAND**-based (black) MIS capacitors. Inset B: AFM image (bottom) of a **2p-SAND** film on Si. (C) Transfer plots and (D) output plots for pentacene OTFTs based on **2p-SAND**.

capacitance of a 300 nm thick SiO<sub>2</sub> dielectric layer ( $\sim 11$  nF/cm<sup>2</sup>). Although the present **p-SAND** capacitances do not benefit from inclusion of a high- $k$  native Al<sub>2</sub>O<sub>3</sub> layer ( $k \approx 9.1$ ), they are comparable to the alkyl SAM phosphonic acid/Al<sub>2</sub>O<sub>3</sub>/Al values reported by Klauk (700 nF/cm<sup>2</sup>)<sup>9a</sup> and Jen (600–760 nF/cm<sup>2</sup>).<sup>9b</sup> From the accumulation regime capacitances and assuming  $d_{\text{native oxide}} = 1.5$  nm and that  $k_{\text{PAE}}, d_{\text{PAE}}(\text{p-SAND}) \approx k_{\text{stb}}, d_{\text{stb}}(\text{SAND, stb} = \text{the SAND stilbazolium unit})$ ,<sup>7</sup> a  $k$  of  $\sim 7$  is derived for the zirconium phosphonate layer and  $\sim 3.6$  for the entire **p-SAND** trilayer (**ZrP** + **PAE** + **ZrP**). Studies of these parameters as a function of self-assembly details and layer density are currently in progress.

Given the excellent **p-SAND** dielectric properties, pentacene OTFTs were next fabricated using **1p-SAND** and **2p-**

**SAND** as the gate dielectrics. Figure 2 shows representative transfer plots for these OTFTs which demonstrate reproducible  $I$ – $V$  characteristics at low operating voltages (less than  $-2$  V). From the  $I$ – $V$  data, the average field-effect mobility is calculated in the saturation regime ( $V_G < V_{DS} = -2$  V) by plotting the square root of the drain current versus gate voltage. These pentacene OTFTs exhibit hole mobilities of  $0.10 \pm 0.02$  and  $0.27 \pm 0.02$  cm<sup>2</sup>/(Vs), and on–off current ratios of  $5 \times 10^3$  and  $3 \times 10^4$  when fabricated on **1p-SAND** and **2p-SAND**, respectively. These parameters are comparable to those of control devices fabricated with a conventional 300 nm thick SiO<sub>2</sub> gate dielectric (mobility  $\approx 0.3$  cm<sup>2</sup>/(V s), see Figure S3 in the Supporting Information). The present results demonstrate that phosphonic-acid-based precursors enable efficient fabrication of OTFT multilayer dielectrics exhibiting high capacitances and low leakage current densities. Moreover, these **p-SAND** materials should be well-suited for self-assembly on the native oxide coatings of Al and Ag contacts as already demonstrated for SAMs,<sup>9</sup> opening possibilities for efficient circuit fabrication.

In summary, the solution-phase deposition of structurally well-defined, high-capacitance, low-leakage multilayer nanodielectrics has been demonstrated under ambient conditions using phosphonic-acid-based precursors. These nanodielectrics can be used for low-operating-voltage pentacene OTFT devices.

**Acknowledgment.** This work was supported by the AFOSR (FA9550-08-1-0331) and the NSF MRSEC program (DMR-0520513) at Northwestern University. We thank Dr. S. Chatopadhyay for helpful discussions.

**Supporting Information Available:** Synthesis and characterization of chromophore, **p-SAND** films, device fabrication details (PDF). This material is available free of charge via the Internet at <http://pubs.acs.org>.

CM8031187